Results in Engineering 27 (2025) 105794

Contents lists available at ScienceDirect

Results in Engineering

journal homepage: www.sciencedirect.com/journal/results-in-engineering

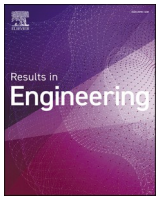

Research paper

Quantitative relation between particle shape and archie's cementation exponent for coarse grains: A statistical analysis

Bosung Choi [a], Jeongwoo Kim [a], Hyunwook Choo [a,c,*], Jongmuk Won [b]

[a] Department of Civil and Environmental Engineering, Hanyang University, Seoul 04763, South Korea
[b] Department of Civil, Urban, Earth, and Environmental Engineering, Ulsan National Institute of Science and Technology (UNIST), Ulsan 44919, South Korea
[c] Developing a team response using digital construction to mitigate disasters related to climate change (BK21 FOUR), Hanyang University, Seoul 04763, South Korea

ARTICLE INFO

Keywords:
Electrical resistivity
Archie's equation
Cementation exponent
Particle shape
Electrical anisotropy

ABSTRACT

The estimation of the cementation exponent (m) in Archie's equation, which is pivotal for interpreting the electrical resistivity of soils and rocks, could be significantly enhanced by correlating it with particle shape characteristics. This study proposes a novel approach in which Archie's m-exponent for sand is estimated based on quantifiable particle shape parameters, including sphericity, convexity, elongation, slenderness, and roundness. The horizontal and vertical electrical resistivities of eight granular materials with varying particle shapes were measured. Correlation matrix scatter plot and multiple linear regression analyses were conducted to establish a quantitative relationship between Archie's m-exponents, electrical anisotropy, and particle shape parameters. The results indicate that all the investigated shape parameters exhibited strong correlations with m-exponents and electrical anisotropy. However, multiple linear regression analysis revealed that roundness (RD) is the most influential shape parameter, likely due to multicollinearity among the other shape parameters. Notably, m-exponents in both the vertical and horizontal directions were found to decrease linearly with increasing RD, as RD effectively captured the tortuosity of the electrical flow paths at a given porosity. These findings are supported by data from previous studies, further validating the observed relationship between RD and electrical properties.

1. Introduction

The electrical resistivity of soils is a critical parameter in various geophysical, environmental, and engineering applications. It plays a vital role in subsurface characterization, groundwater exploration, and the assessment of sedimentary environments [1–8]. Archie's equation [9] expresses a fundamental relationship between the electrical resistivity of saturated porous materials and their porosity, which has been widely employed in previous studies to estimate hydrocarbon reserves, aquifer properties, and other subsurface characteristics [10–16]. Archie's equation describes how the electrical resistivity (ρ_{mix}) of saturated soil can be predicted based on its porosity (n) and the resistivity of the pore fluid (ρ_w), establishing an essential connection between the physical properties of the soil and its electrical behavior. Numerous studies have demonstrated the relevance of Archie's equation for describing the electrical resistivity of pore water conduction-dominant soils, such as sand and marine clays [17], underscoring its importance in geotechnical and environmental engineering contexts.

The original Archie's equation for saturated soils can be expressed as

$$\rho_{mix} = \rho_w \cdot n^{-m} \tag{1}$$

where m is the cementation exponent (or factor) or Archie's m-exponent. Archie also defined the formation factor (F) to isolate the impact of pore fluid on the electrical properties of soils:

$$F = \frac{\rho_{mix}}{\rho_w} = n^{-m} \tag{2}$$

Eqs. (1) and (2) highlight that the m-exponent is the key parameter for the reliable estimation of the porosity (n) of the tested soil or the pore fluid concentration based on the measured electrical resistivity. The m-exponent is a dimensionless parameter that reflects the complexity of the pore structure and connectivity of the pore spaces within the sediment matrix, which can be reflected by the arrangement and geometry of soil particles. Traditionally, the m-exponent has been considered to depend primarily on the porosity and degree of cementation in the material; thus, it was called the cementation exponent (or factor) [9].

* Corresponding author.
E-mail addresses: bosung123@hanyang.ac.kr (B. Choi), kimjeongwoo@hanyang.ac.kr (J. Kim), choohw@hanyang.ac.kr (H. Choo), jwon@unist.ac.kr (J. Won).

https://doi.org/10.1016/j.rineng.2025.105794
Received 24 January 2025; Received in revised form 20 May 2025; Accepted 14 June 2025
Available online 14 June 2025

However, later studies [15,18] revealed that the *m*-exponent is more closely related to the particle or pore shape; thus, the *m*-exponent is also called the shape factor.

The shape of sand particles plays a crucial role in determining the physicomechanical properties of sandy soils [6,19–24]. These include the fabric, packing density, strength, stiffness, compressibility, and various conduction properties, such as electrical, hydraulic, and thermal conductivity. For instance, angular particles enhance the soil fabric through increased interlocking, leading to higher shear strength owing to improved frictional resistance [25]. Similarly, angular or elongated particles contribute to greater small-strain stiffness and reduced stress dependency [26,27]. Conduction properties are also influenced by particle shape, as it affects the packing density, pore space connectivity, and tortuosity [28–30], all of which are critical factors in determining conductivity.

Despite the acknowledged importance of particle shape in governing soil conduction properties, its specific effect on the *m*-exponent in Archie's equation remains largely unexplored. Previous research has established that the *m*-exponent for sand generally falls between 1.3 and 1.8, with elongated or platy particles exhibiting higher values due to increased tortuosity and longer electrical conduction paths [30–33]; however, a comprehensive understanding is lacking. Studies focusing on sphericity or elongation have dominated the literature, neglecting the influence of other crucial shape parameters, such as convexity, slenderness, and roundness. Notably, some physicomechanical properties of sandy soils, such as packing density and friction angle, are more effectively quantified by angularity (or roundness) than by sphericity [25]. Furthermore, the quantitative relationship between these diverse shape parameters and the *m*-exponent has received minimal attention. This knowledge gap highlights the need for further research to systematically investigate the influence of a broader range of particle shape parameters, including sphericity, convexity, elongation, slenderness, and roundness, on Archie's *m*-exponent.

This study investigated the horizontal and vertical electrical resistivities of eight granular materials with varying particle shapes. The research focused on examining the variations in Archie's *m*-exponents in the vertical and horizontal directions, as well as the electrical anisotropy in relation to different particle shape parameters. To establish a quantitative relationship between Archie's *m*-exponents, electrical anisotropy, and particle shape parameters, the study used a correlation matrix scatter plot and multiple linear regression analyses.

2. Experimental program

2.1. Materials

Eight different types of granular materials, including seven sands and one type of glass beads with varying particle shapes, were used in this study to investigate the influence of particle shape on the electrical properties of coarse-grained soils (Fig. 1). The seven sands consist of both artificially crushed and natural sands. The artificially crushed sands include K-5 and K-6 sands, both supplied by Kyung In Material Company (South Korea). The natural sands include Jumunjin sand, sourced near the Jumunjin Coast (South Korea) and supplied by Jumunjin Silica Company; Nakdong sand, collected near the Nakdong River (South Korea) and supplied by Northern Aggregate Company; South-Han sand, obtained near the South Han River (South Korea) and supplied by Shinpyeong Aggregate Company; Ottawa sand, a standardized silica sand (ASTM C778 compliant) sourced from Ottawa, Illinois (USA) and supplied by U.S. Silica Company; and Hiroshima sand, collected from the Hiroshima region (Japan) and supplied by Sakohiro Crushed Stone Company. The glass beads were supplied by Korea Ace Scientific Company, South Korea. The index properties of the tested materials are listed in Table 1. The uniformity coefficient (C_u) of the samples used to investigate the influence of particle shape on electrical properties ranged from 1.00 to 2.14, as presented in Table 1. This variation reflects distinct particle size distributions among the samples; however, all materials are classified as poorly graded sand according to the Unified Soil Classification System (USCS).

Table 1
Index properties of tested materials.

Type		G_s	D_{50} (mm)	C_u	e_{max}	e_{min}
Particle shape effect	K-5	2.65	0.77	1.88	1.05	0.69
	K-6	2.65	0.42	1.85	1.04	0.66
	Jumunjin	2.60	0.53	1.90	0.85	0.60
	Nakdong	2.66	0.45	2.14	1.05	0.77
	Ottawa	2.65	0.61	1.48	0.74	0.50
	Hiroshima	2.60	0.39	1.63	0.94	0.66
	South-Han	2.61	0.43	2.96	0.94	0.66
	Glass beads	2.46	1.00	1.00	0.61	0.48
Gradation effect	Well-graded Glass beads	2.46	0.85	4.78	0.55	0.42

Note: G_s = specific gravity (ASTM D854); D_{50} = median particle size (ASTM D422); C_u = uniformity coefficient; e_{max} = maximum void ratio (ASTM D4254); e_{min} = minimum void ratio (ASTM D4253).

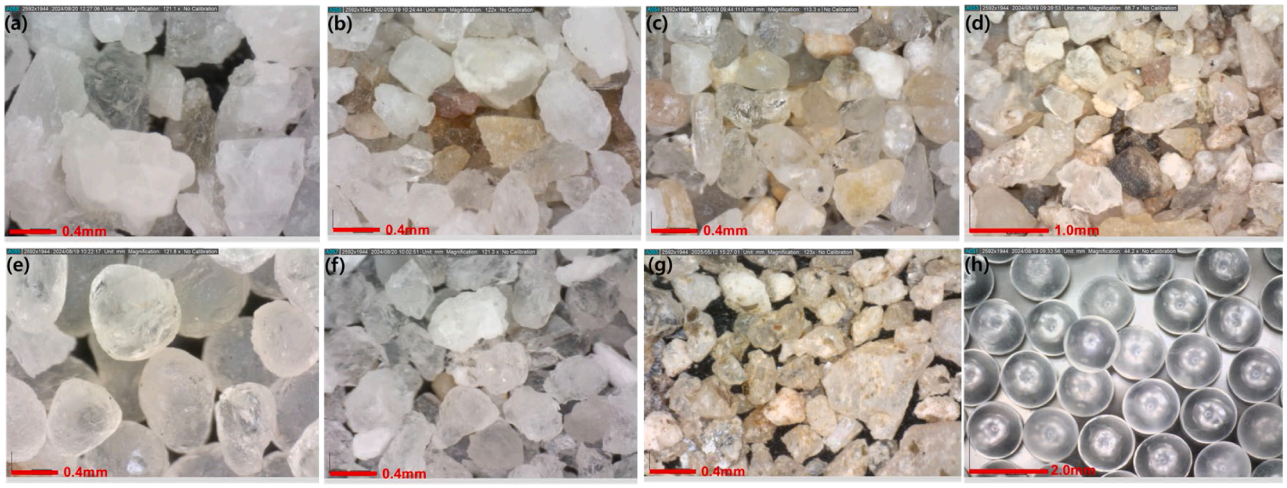

Fig. 1. The optical images of the tested materials: (a) K-5 sand, (b) K-6 sand, (c) Jumunjin sand, (d) Nakdong sand, (e) Ottawa sand, (f) Hiroshima sand, (g) South-Han sand and (h) glass beads.

2.2. Quantification of particle shape parameters

Five particle shape parameters: sphericity (SP), convexity (CX), elongation (EG), slenderness (SD), and roundness (RD), were used to investigate the effect of particle shape on the electrical resistivity of sands. The quantitative definitions of these five particle shape parameters are shown in Fig. 2. The SP assesses how closely the shape a particle resembles an ideal sphere, as it depends on both the overall form and degree of roundness, with a perfect sphere having equal dimensions and complete roundness [34,35]. CX is defined as the ratio of the area of the particle to the area of its convex hull and serves as an indicator of particle angularity [36,37]. Both EG and SD describe the extent to which the particles are stretched; however, their definitions differ. EG is the ratio of the longest to the shortest distance from the centroid to the particle surface, while SD is the ratio of the length of the longest axis to the shortest axis of a fitted ellipse [38–40]. RD, defined by Wadell [41], describes the edge (or corner) characteristics of the particle and can be defined as the ratio of the average radius of curvature of the edges of the particle to the radius of the largest inscribed circle that can fit within the particle (Fig. 2).

The five particle shape parameters for each material were calculated from microscope images obtained using a digital microscope (Leica DMC2900) at magnifications ranging from 30 × to 60 × . Representative oven-dried subsamples were evenly spread on a clean glass slide to minimize particle overlap and ensure accurate boundary detection. A total of 200 images were captured for each material, and approximately 5–8 individual particles were analyzed in each image. The images were binarized and processed using ImageJ software, where particle boundaries were detected and shape descriptors such as aspect ratio, circularity, and roundness were computed. To ensure data quality, outliers in roundness values were identified and removed using a standard threshold of mean± 3 standard deviations (3σ), resulting in the removal of fewer than five data points per sample. Since all shape parameters were dimensionless and exhibited comparable value ranges, data normalization was not applied. Table 2 summarizes the computed particle shape parameters for the eight tested materials.

To provide an independent validation of the ImageJ-derived shape parameters, additional measurements of slenderness and sphericity were conducted using a laser diffraction system (BeVision D2, Bettersize Instrument Ltd). The comparison showed strong agreement in slenderness values between the two methods, with a maximum difference of <2 % (Figure S1 in the supplementary material), thereby increasing the reliability of ImageJ-derived shape parameters. However, sphericity values were not compared due to fundamental differences in the definitions and calculation methods used by ImageJ and the laser diffraction system.

Table 2
Determined particle shape parameters of tested materials.

Type	SP	CX	EG	SD	RD
K-5	0.805	0.969	1.766	1.511	0.270
	(0.051)	(0.014)	(0.350)	(0.619)	(0.052)
K-6	0.797	0.959	1.847	1.584	0.330
	(0.042)	(0.021)	(0.259)	(0.202)	(0.104)
Jumunjin	0.783	0.965	1.955	1.440	0.484
	(0.066)	(0.016)	(0.479)	(0.515)	(0.049)
Nakdong	0.779	0.951	1.996	1.473	0.298
	(0.072)	(0.026)	(0.496)	(0.625)	(0.076)
Ottawa	0.866	0.986	1.440	1.342	0.739
	(0.042)	(0.006)	(0.191)	(0.560)	(0.093)
Hiroshima	0.778	0.947	2.008	1.538	0.424
	(0.066)	(0.031)	(0.511)	(0.366)	(0.093)
South-Han	0.813	0.968	1.823	1.431	0.312
	(0.068)	(0.016)	(0.399)	(0.283)	(0.072)
Glass beads	1.000	1.000	1.000	1.000	1.000

Note, number in parentheses = standard deviation.

2.3. Sample preparation and measurement

To prepare fully saturated specimens, the water pluviation method was employed in this study. The initial relative densities of each specimen were set to 30 % and 60 % by applying symmetric tapping. Subsequently, a vertical stress of up to 363.3 kPa was applied to the specimens to determine the variation in electrical resistivity across a wide range of porosities. Because the tested sands/glass beads contained no fine particles passing through the #200 sieve, pore water conduction (i.e., ionic conduction through the continuous pore network) governed the overall electrical conductivity (or resistivity) of the tested materials [42]. However, to minimize the potential impact of surface conduction (i.e., a special form of ionic conduction through the particle-pore fluid interface) on Archie's *m*-exponent, high-salinity water (0.5 M NaCl solution) was used as the pore fluid in this study.

To measure the vertical and horizontal electrical resistance, two pairs of four-electrode conductivity probes were installed in the

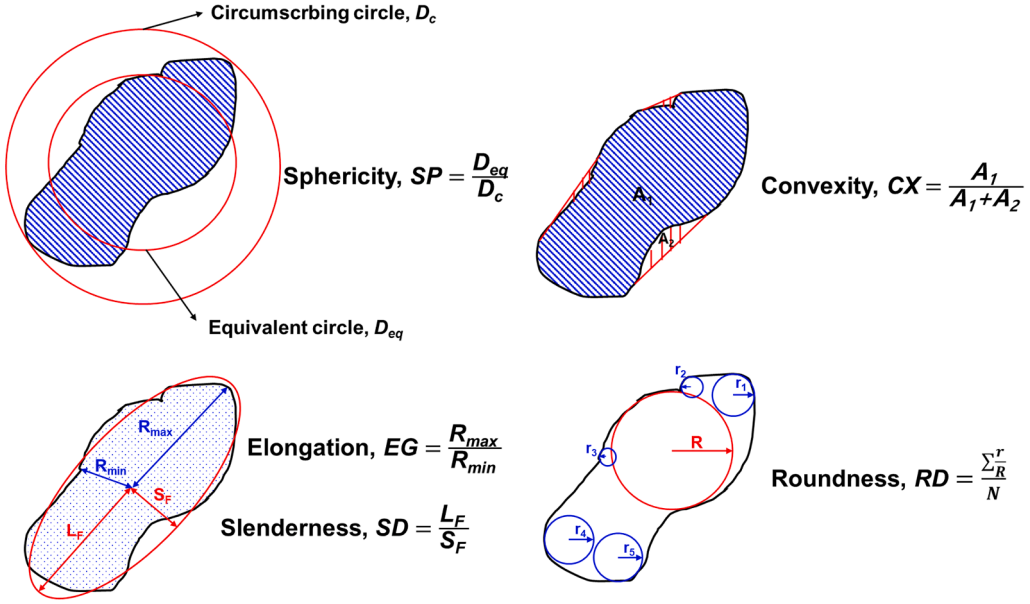

Fig. 2. Definition of particle shape parameters (sphericity, convexity, elongation, slenderness, roundness).

modified oedometer cell (Fig. 3). During the experiment, the electrical flow through the soil traveled from the high-current electrode (Hc) to the low-current electrode (Lc), and the electrical resistance between the two potential electrodes (Hp and Lp) was measured using an LCR meter (E4980AL, Keysight). The input voltage of the LCR meter was set to 1 V. An operating frequency of 10 kHz was selected to avoid electrical resonance and electrode polarization. As mentioned above, vertical stresses ranging from 13.5 kPa to 363.3 kPa were applied to the test specimen, and electrical resistance measurements were conducted at the end of each loading step. The measured resistance was converted into electrical resistivity using the calibration factor, which was determined by measuring both the electrical resistance and resistivity of NaCl solutions with varying concentrations (Fig. 3). All measurements were conducted at a controlled room temperature of approximately 23 °C (±1 °C) to ensure consistency across tests and to eliminate potential thermal effects on the results.

3. Results and discussion

3.1. Measured electrical resistivity

Figs. 4(a) and (b) show the variations in the formation factor in the vertical (F_v) and horizontal (F_h) directions according to porosity (n). Note that the formation factor was defined in Eq. (2) as the ratio between the measured bulk electrical resistivity (ρ_{mix}) and pore water resistivity (ρ_w). With a decrease in n (or void ratio), both F_v and F_h of all tested materials increased owing to the increase in ρ_{mix}, resulting from the decrease in the number and size of channels for current flow [11,12,43,44]. Because most soils particles are electrically nonconductive, this observation confirms that the pore water conduction is the dominant mechanism determining the overall resistivity or conductivity of tested materials. Stated another way, a lower n implies fewer and/or smaller pore spaces, which restricts the flow of electrical current and increases the overall resistivity of the tested materials, thus increasing F. Figures 4 (a) and (b) also demonstrate that the tested materials showed varying Archie's m-exponents, ranging from 1.35 to 1.82 in the case of F_v, and from 1.33 to 1.70 in the case of F_h, reflecting the effect of electrical anisotropy. The varying m-exponents can be attributed to the particle shapes of the tested materials, which will be discussed later.

3.2. Electrical anisotropy

Figure 4(c) shows the electrical anisotropy (λ_e) according to the porosity (n) for the tested eight granular materials. The λ_e can be defined as [15]

$$\lambda_e = \sqrt{\rho_{mix,\,v}/\rho_{mix,\,h}} = \sqrt{F_v/F_h} \tag{3}$$

where $\rho_{mix,v}$ and $\rho_{mix,h}$ are the electrical resistivities in the vertical and horizontal direction, respectively. The determined λ_e values of all tested materials were greater than 1, indicating that the electrical resistivity in vertical direction is always greater than that in horizontal direction due to the anisotropic nature of soil structure. Because soil particles tend to align preferentially in the horizontal direction during deposition, the pore connectivity in the horizontal direction is better than that in the vertical direction. Thus, the electrical current flowed more easily in the horizontal direction, while the vertical direction flow was more tortuous. Many previous studies also reported than λ_e ranged from 1 to 2 [15,45,46].

At first glance, Figure 4(c) appears to demonstrate a linear relationship between the n and λ_e of the tested materials. However, upon closer examination of individual soil samples, it becomes evident that there was no distinct relationship between the two parameters. The extreme void ratios of sandy soils are determined primarily by the particle shape (Fig. 5) [25,47]. Consequently, the observed variations in λ_e with respect to n in Figure 4(c) are indicative of changes in electrical anisotropy due to particle shape rather than porosity. Finally, it is notable that the maximum λ_e of tested materials was approximately 1.05, indicating that poorly graded sand can have up to approximately 10 % greater electrical resistivity in vertical direction than that in horizontal direction.

3.3. Correlation matrix

Fig. 6 illustrates the scatter plot matrix of all the dependent and independent variables, including least-squares fitted lines, Pearson correlation coefficients (ρ), p-values (p), and the coefficient of determination (R^2). The correlation plots in the first column show the correlation between the determined Archie's m-exponent in the vertical direction (m_v) and the individual parameters that potentially influence m_v values. Similarly, the correlation plots in the second column show the correlation between Archie's m-exponent in the horizontal direction (m_h) and the individual parameters that potentially influence m_h values. The correlation plots between electrical anisotropy (λ_e) and the five different shape parameters are shown in the third column of Fig. 6.

m_v, m_h, and λ_e showed negative correlations ($\rho < 1$) for roundness (RD), sphericity (SP), and convexity (CX) and positive correlations ($\rho > 1$) for elongation (EG) and slenderness (SD) (Fig. 6). Thus, with increasing RD, SP, and CX, and decreasing EG and SD, the electrical current encounters less resistance and anisotropic pore structure when flowing through the pore space between soil particles, leading to a

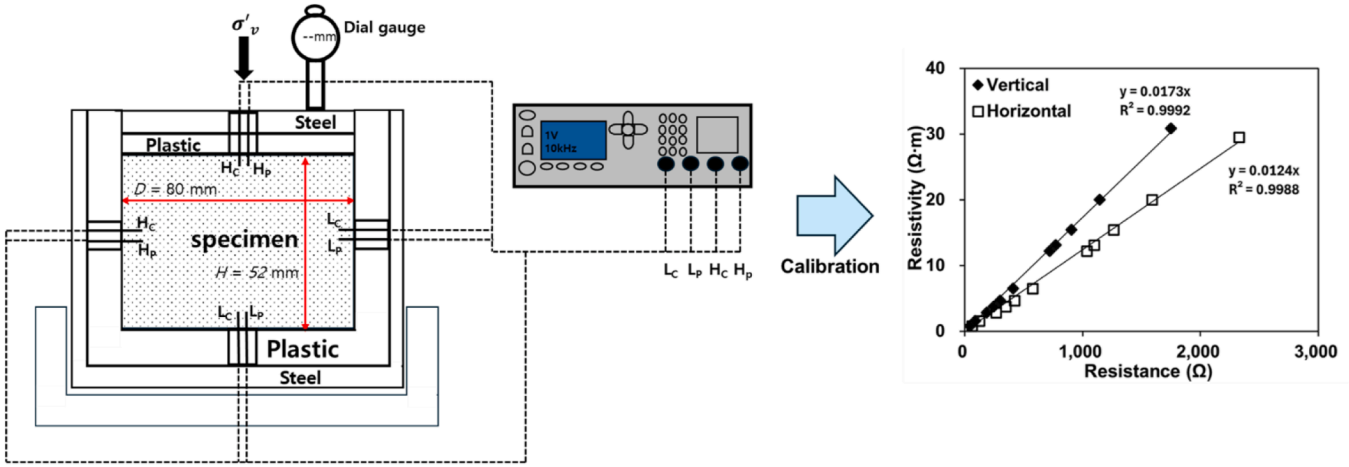

Fig. 3. Test setup for electrical resistivity measurements.

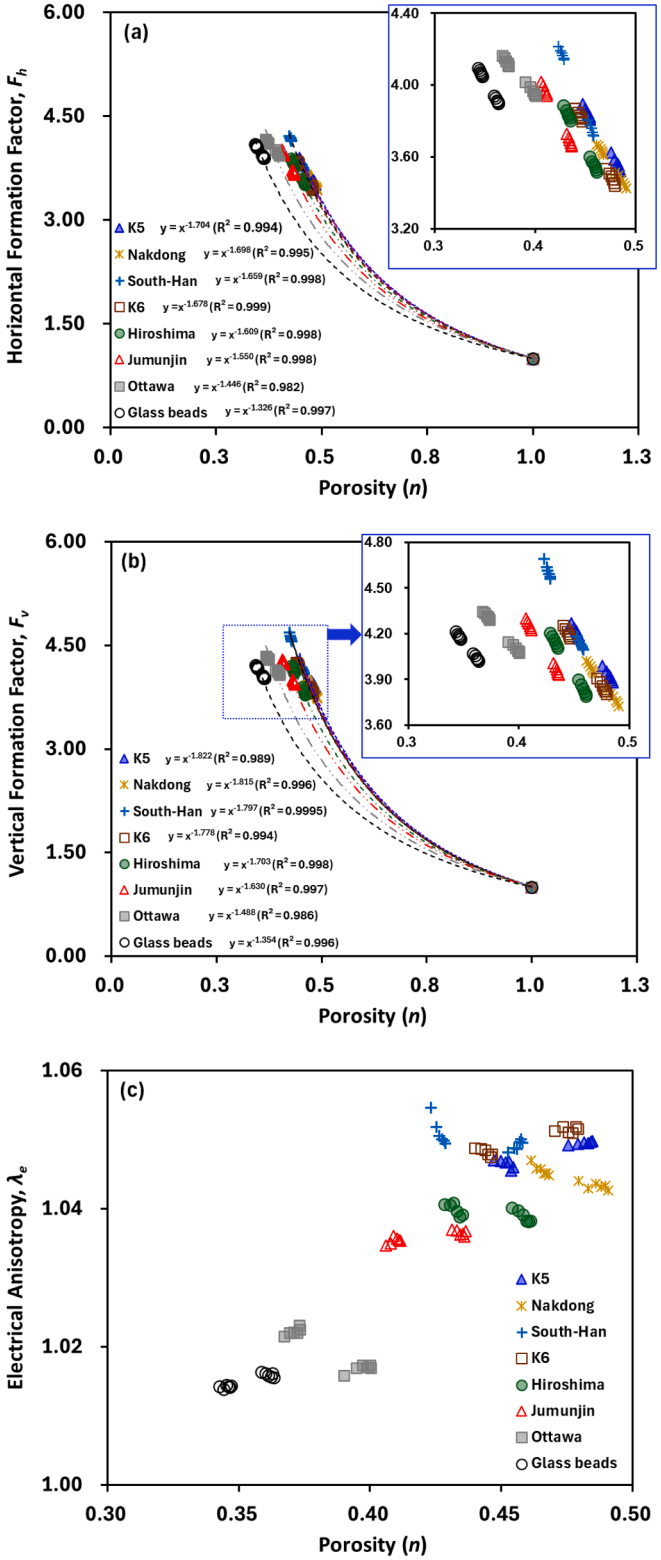

Fig. 4. Variations of (a) formation factor in vertical direction (F_v); (b) formation factor in horizontal direction (F_h); and (c) electrical anisotropy according to porosity.

smaller Archie's m-exponent and λ_e. In other words, angular or elongated particles can create more tortuous pathways for fluid flow, potentially decreasing the hydraulic/electrical conductivity and consequently increasing the m-exponent. By contrast, rounded/spherical particles may enhance direct flow paths, leading to an increase in the

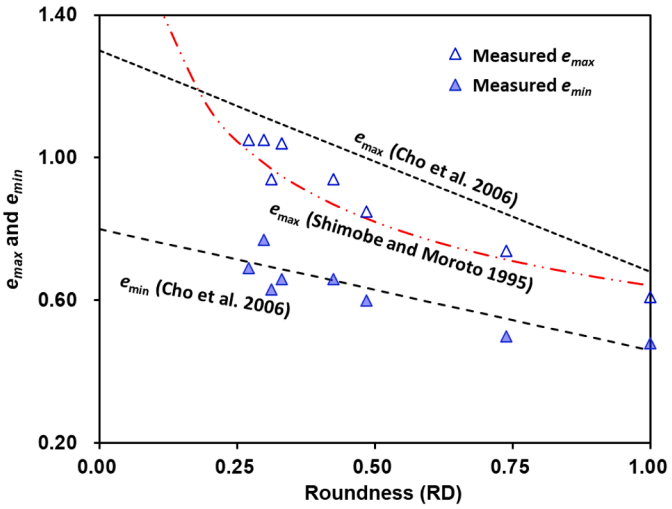

Fig. 5. Variations of maximum and minimum void ratios (e_{max} and e_{min}) according to roundness (RD).

hydraulic/electrical conductivity and consequently decreasing the m-exponent [28,30,48,49]. The order of absolute ρ and R^2 values of RD > SP > SD > EG > CX for both m_v and m_h indicates that RD is the most strongly correlated parameter for estimating Archie's m-exponent of tested materials. The order of absolute ρ and R^2 values of RD > SD > SP > EG > CX for λ_e indicates that RD is the most strongly correlated parameter for estimating λ_e of tested materials. However, the p-values for individual shape parameters for estimating m_v, m_h, and λ_e suggest that all shape parameters are statistically significant at the conventional 0.05 level.

Strong positive correlations occur between m_v and m_h, and between m_v (or m_h) and λ_e ($\rho > 0.97$ and $R^2 > 0.95$) (Fig. 6). Because both m_v and m_h are affected by the same particle shape parameters in a similar manner, a direct relationship between m_v and m_h can be expected. Based on Eq. (3), λ_e should increase with increasing difference between m_v and m_h. Although the ratio between m_v and m_h is approximately constant regardless of m_v (or m_h) values (Fig. 6), the difference between m_v and m_h increases with increasing m_v (or m_h) values. Thus, λ_e nearly linearly increased with increasing m_v (or m_h). Salem and Chilingarian [15] also reported a linear relationship between Archie's m-exponent and λ_e.

Fig. 6 also demonstrates that the five shape parameters employed in this study were strongly correlated. As mentioned earlier, both the EG and SD parameters capture similar concepts regarding the extent of the elongation of the particle. The consequent strong correlation between EG and SD is shown in Fig. 6. As the convex hull used to determine the CX (Fig. 2) of a circle is identical to the circle itself, the concept of CX is similar to that of SP, leading to the strong correlation between CX and SP, as shown in Fig. 6. Lee et al. [23] demonstrated that SP can be correlated with SD and EG, which indicates that EG, SD, CX, and SP are interrelated. Moreover, RD is strongly correlated with the other shape parameters (Fig. 6). RD reflects the degree of smoothness and curvature of the edges of a particle, which are closely related with SP and CX. In addition, elongated or slender particles typically have sharper edges and less smooth surfaces, resulting in an inverse relationship between RD and EG (or SD). Consequently, strong correlations were observed among the five shape parameters employed in this study.

3.4. Multiple linear regression analysis

This section quantitatively investigates the relationship between Archie's m-exponent (both m_v and m_h) and electrical anisotropy (λ_e) with particle shape parameters. Multiple linear regression analysis was conducted using the statistical software R, incorporating the five shape parameters (RD, SP, CX, EG, and SD). Thus, m_v, m_h, and λ_e can be

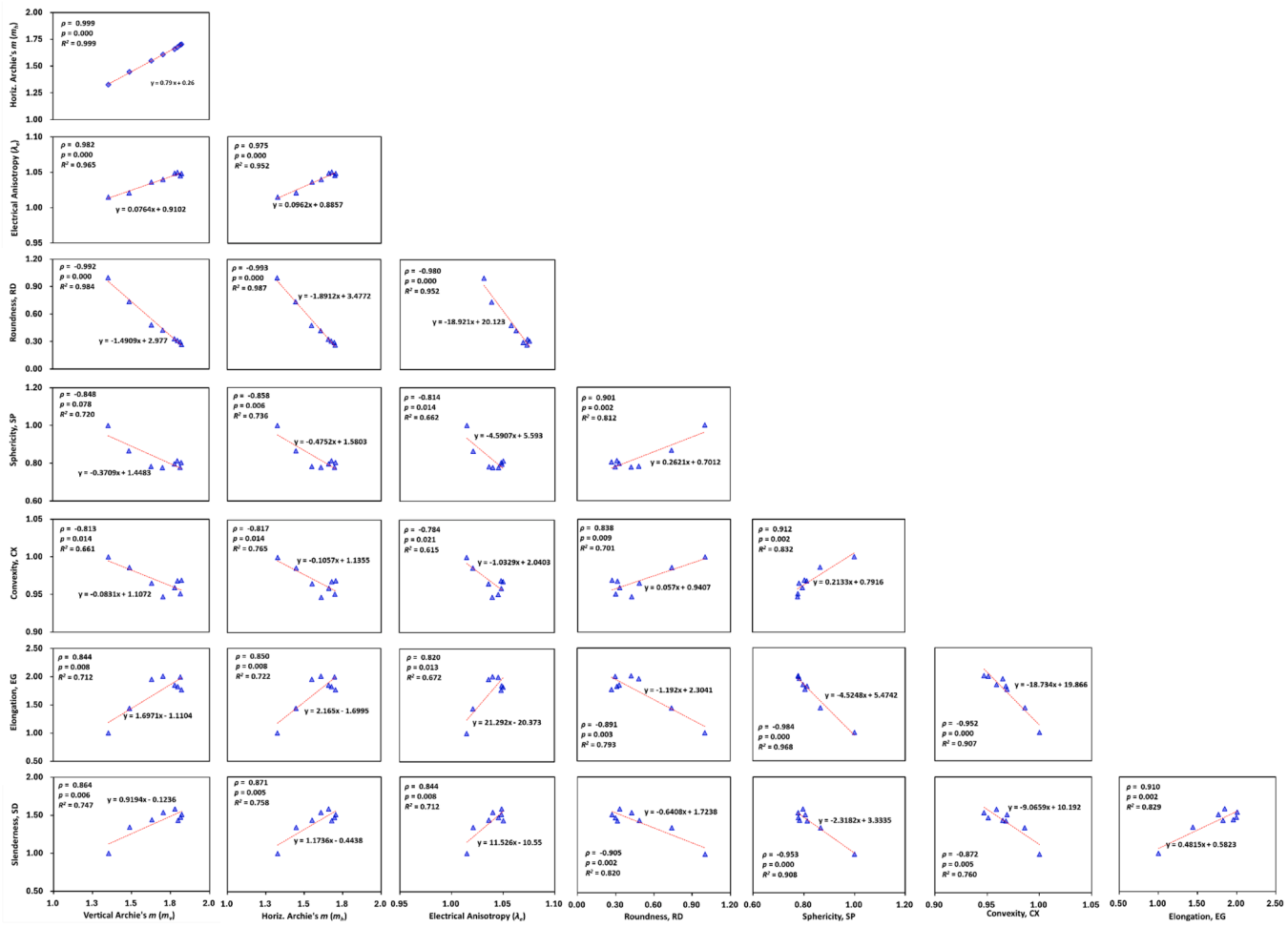

Fig. 6. Correlation matrix scatter plot of all the dependent and independent variables employed in this study with least-squared fitted lines: ρ = Pearson coefficient, p = p-value, R^2 = Coefficient of determination.

Table 3
Coefficients, p-values, and R-square values for multiple regression analysis.

Type	Coefficient						R^2
		RD	SP	CX	EG	SD	
	a_1	a_2	a_3	a_4	a_5	a_6	
m_v	6.062	−0.830	−0.432	−2.979	−0.280	−0.186	0.999
	(0.050)	(0.001)	(0.477)	(0.064)	(0.126)	(0.169)	
	1.442	−0.694		0.585			0.980
	(0.173)	(0.000)		(0.571)			
	1.992	−0.660					0.984
	(0.000)	(0.000)					
	b_1	b_2	b_3	b_4	b_5	b_6	
m_h	6.811	−0.654	−1.145	−3.059	−0.372	−0.254	0.999
	(0.022)	(0.001)	(0.088)	(0.034)	(0.044)	(0.059)	
	1.441	−0.546		0.419			0.987
	(0.083)	(0.000)		(0.579)			
	1.835	−0.522					0.986
	(0.000)	(0.000)					
	c_1	c_2	c_3	c_4	c_5	c_6	
λ_e	0.123	−0.056	0.427	0.387	0.077	0.058	0.999
	(0.594)	(0.005)	(0.025)	(0.072)	(0.038)	(0.042)	
	0.983	−0.055		0.084			0.956
	(0.001)	(0.002)		(0.546)			
	1.062	−0.050					0.952
	(0.000)	(0.000)					

Note, number in parentheses = p-value. RD = roundness; SP = sphericity; CX = convexity; EG = elongation; and SD = slenderness.

expressed as

$$\begin{aligned} m_v &= a_1 + a_2 \cdot RD + a_3 \cdot SP + a_4 \cdot CX + a_5 \cdot EG + a_6 \cdot SD \\ m_h &= b_1 + b_2 \cdot RD + b_3 \cdot SP + b_4 \cdot CX + b_5 \cdot EG + b_6 \cdot SD \\ \lambda_e &= c_1 + c_2 \cdot RD + c_3 \cdot SP + c_4 \cdot CX + c_5 \cdot EG + c_6 \cdot SD \end{aligned} \quad (4)$$

where *a, b*, and *c* are fitting (or regression) coefficients.

The fitted coefficients for Eq. (4) are listed in Table 3, and the numbers in parentheses in Table 3 indicate p-values. The resulting models for m_v, m_h, and λ_e were robust with an R^2 of over 0.99 (Table 3), suggesting a strong correlation between the employed particle shape parameters and the measured electrical properties. However, although the overall models exhibited excellent predictive power, an examination of the significance of the individual parameters revealed a nuanced picture. Statistical analysis indicated that only RD demonstrated a statistically significant ($p < 0.05$) influence on m_v, m_h, and λ_e, while the other shape parameters (SP, CX, EG, and SD) exhibited nonsignificant p-values ($p > 0.05$). This suggests that, although the collective effect of all shape parameters is substantial, RD is the primary shape parameter driving the variations in the m_v, m_h, and λ_e within this dataset.

To further investigate the above findings, multicollinearity among the independent variables was assessed by computing the variance inflation factors (VIF) using the regression software R. VIF analysis revealed significant multicollinearity, with most shape parameters displaying VIF values far above the commonly accepted threshold of 10, except for RD (VIF = 7.5). Specifically, SP, CX, EG, and SD exhibited extremely high VIF values (SP = 238.9, CX = 41.8, EG = 120.3, and SD = 152), indicating a high degree of correlation among these variables. Such multicollinearity inflates the variance of the regression coefficients and can obscure the individual contributions of each parameter, which explains why SP, CX, EG, and SD had nonsignificant p-values in the regression model. While the regression model captures the overall influence of the particle shape on the electrical properties, the strong interdependence among these variables makes it difficult to isolate their individual effects.

Three independent variables with the highest VIF values were eliminated, and the remaining two variables (RD and CX) were used to perform additional multiple linear regression analyses (Table 3). Thus, m_v, m_h, and λ_e can be expressed as

$$\begin{aligned} m_v &= a_1 + a_2 \cdot RD + a_4 \cdot CX \\ m_h &= b_1 + b_2 \cdot RD + b_4 \cdot CX \\ \lambda_e &= c_1 + c_2 \cdot RD + c_4 \cdot CX \end{aligned} \quad (5)$$

The comparison of predictive models between Eqs. (4) and (5) demonstrate that the R^2 values decreased slightly, while the p-value of CX increased significantly (Table 3), indicating that CX can also be excluded from the variable in the predictive model of Eq. (5). Therefore, a simplified model was developed with RD as the sole predictor:

$$\begin{aligned} m_v &= a_1 + a_2 \cdot RD \\ m_h &= b_1 + b_2 \cdot RD \\ \lambda_e &= c_1 + c_2 \cdot RD \end{aligned} \quad (6)$$

Despite the reduction in the number of variables, Eq. (6) still demonstrated strong predictive power, with R^2 values exceeding 0.95 (Table 3), comparable to the more complex models. This indicates that RD alone is sufficient to reliably estimate Archie's *m*-exponents and the electrical anisotropy (λ_e) for the dataset.

In summary, although the initial model incorporating all five shape parameters provided excellent predictive accuracy, multicollinearity among the parameters, particularly SP, CX, EG, and SD, obscured their individual contributions. After addressing multicollinearity, RD emerged as the dominant factor influencing the electrical properties, allowing for a simpler and more interpretable model that retained strong predictive performance.

3.5. Electrical properties and roundness of sand

The particle shape of sand plays a critical role in determining the tortuosity of the flow path, which influences the connectivity of the pore space and path for electrical conduction in sand [49]. Among the shape parameters employed in this study, RD exhibited the most significant impact on Archie's *m*-exponents and λ_e, suggesting that RD is the most influential factor in determining the flow path in sand. This highlights the importance of RD in shaping the tortuosity and electrical conduction behavior of granular materials. RD refers to the smoothness of the edges and corners of a particle (Fig. 2), indicating that RD can reflect the local pore structure and flow path. Higher RD values (rounder particles) tend to create larger, more interconnected pores with smoother flow paths, while lower RD values (more angular particles) result in smaller, more constricted pores with sharper edges and corners, increasing flow path tortuosity. Therefore, RD can detect the obstruction for electrical current flow in porous media, leading to RD that strongly reflects Archie's *m*-exponent. By contrast, other shape parameters (SP, CX, EG, and SD) are determined by the overall particle shape (Fig. 2); thus, information regarding the characteristics of the local pore structure and the consequent tortuosity of the electrical conduction path is limited in SP, CX, EG, and SD.

These observations can be better understood from a microscale perspective. The tortuosity of the electrical conduction path, defined as the curvature or complexity of flow paths between soil particles, plays a pivotal role in determining bulk electrical resistivity and is conceptually illustrated in Fig. 7 (a schematic showing tortuous paths in angular vs. rounded grains) and expressed by Eq. (7) [11]:

$$T_e = F \cdot n = n^{1-m} \quad (7)$$

where T_e = electrical tortuosity ($T_e = (L_e / L)^2$, where L_e and L are defined in Fig. 7. Most importantly, Eq. (7) highlights that soils with larger *m*-exponents exhibit greater electrical tortuosity.

Fig. 8 shows the calculated T_e of tested materials based on Eq. (7) according to porosity (n). As n decreases, the available conduction paths become increasingly narrow and irregular, leading to a higher formation factor and an increase in T_e [50]. Importantly, particle shape influences this tortuosity by modulating the geometry and connectivity of the pore space. Angular or elongated particles tend to create more complex and indirect conduction paths, whereas rounded particles contribute to the formation of smoother and more continuous pore networks (Fig. 7). These microscale structural differences ultimately govern the ease with which electrical current flows through the saturated granular medium. Thus, T_e at a given porosity increases with increasing angularity of particles (Fig. 8). This trend is further supported by a comparison with the classical Maxwell equation, which assumes idealized spherical inclusions in a conductive medium. The Maxwell equation for T_e of nonconducting spheres can be expressed as [51]:

$$T_e = 1 + 0.5 \cdot (1 - n) \quad (8)$$

Tested rounded (or spherical) particles exhibited behavior closely matching Maxwell's predictions, while more angular (or elongated) particles showed increasing deviation (Fig. 8), indicating enhanced electrical tortuosity and more convoluted conduction paths in the pore structure. These findings support that the regression coefficients derived from particle shape parameters are not only statistically significant but also physically meaningful, as they reflect the degree of electrical tortuosity governed by pore structure geometry.

Finally, to verify the quantitative relationship between the electrical properties and RD suggested in this study, data from previous studies [31,30,33] were used. Notably, most previous studies measured only the horizontal electrical resistivity; therefore, the relationship between m_h and RD was validated using these previous experimental results. Fig. 9 presents the relationship between m_h and RD, as shown in Fig. 6 and Table 3, along with data from the aforementioned studies. Because many

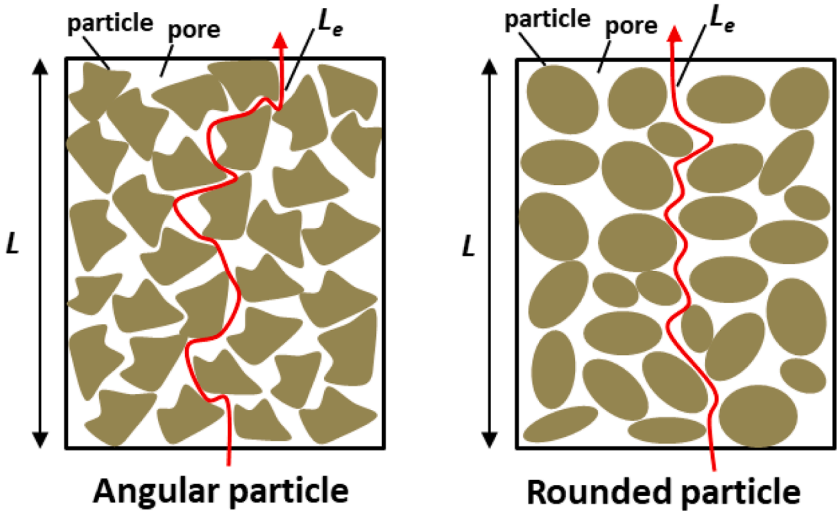

Fig. 7. Schematic drawing of electrical conduction path for angular and rounded particles. Note, L = straight length and L_e = length of electrical conduction path.

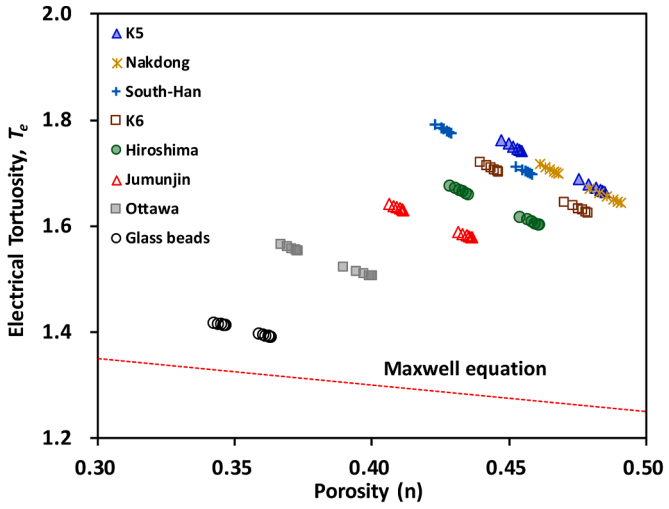

Fig. 8. Variation of electrical tortuosity (Eq. (7)) according to porosity. Note, Maxwell equation = Eq. (8).

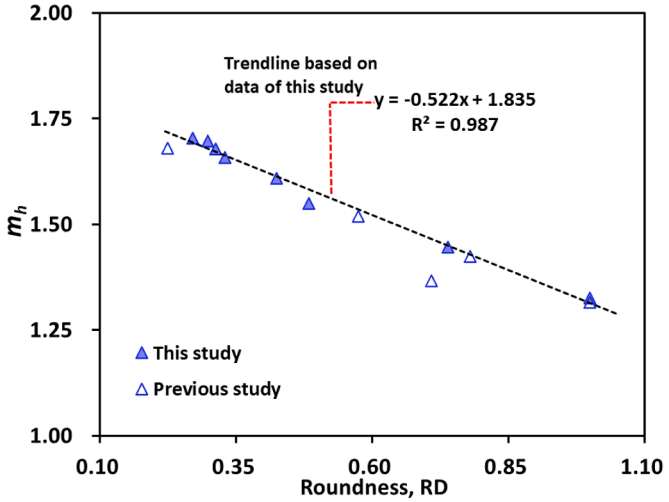

Fig. 9. Variation of Archie's m-exponent in horizontal direction (m_h) according to according to roundness (RD).

previous studies did not provide detailed particle shape information (i.e., RD) or optical images of sand particles, the data points available for model validation were limited. Nevertheless, Fig. 9 demonstrates that the data points from previous studies also aligned with the trend developed in this study, reinforcing the ability of RD to accurately characterize the m-exponent of sand. The mean absolute percentage error (MAPE) was determined to be 1.94 % (<5 %, indicating an acceptably accurate prediction).

3.6. Impact of particle gradation on Archie's m-exponent

To investigate the potential impact of particle gradation on Archie's m-exponent, additional experiments were conducted using well-graded glass beads. The index properties of the well-graded glass beads are provided in Table 1. Unlike the poorly graded sands or glass beads used in the primary experiments, these well-graded samples had a broader distribution of particle sizes. Well-graded glass beads were selected to maintain a relatively consistent mineralogy and surface texture with the poorly graded glass beads, allowing the effect of particle size distribution to be isolated.

The results of the experiments on well-graded glass beads showed that increasing the range of particle sizes led to a decrease in porosity

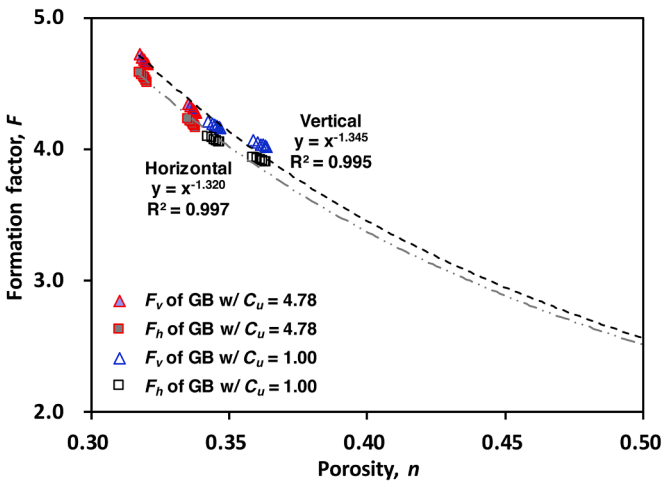

Fig. 10. Effect of particle gradation on the relation between formation factor and porosity. Note, F_v = formation factor in vertical direction; F_h = formation factor in horizontal direction; GB = Glass beads; and C_u = uniformity coefficient.

and a corresponding increase in formation factor or electrical resistivity (Fig. 10). This observation aligns with the understanding that a wider range of particle sizes allows for more efficient packing, thereby reducing the void space within the material. However, despite the changes in porosity and resistivity, the Archie's *m*-exponent was not significantly affected by the change in gradation. The *m*-exponent values for the well-graded glass beads were consistent with those observed for the poorly graded glass beads with similar particle shapes. These findings suggest that while particle gradation influences the overall electrical resistivity of the granular material primarily through its effect on porosity, it does not appear to have a substantial impact on the fundamental relationship between particle shape and Archie's *m*-exponent. This supports the interpretation that Archie's *m*-exponent is more closely related to the geometry and connectivity of the pore space, which is predominantly controlled by particle shape, rather than by the specific distribution of particle sizes, at least within the range of materials tested in this study.

4. Conclusion and recommendation

This study aimed to address the lack of quantitative understanding of how diverse particle shape parameters influence Archie's *m*-exponent (or cementation exponent) and electrical anisotropy in sandy soils. To achieve this, a comprehensive set of shape descriptors, including sphericity (SP), convexity (CX), elongation (EG), slenderness (SD), and roundness (RD), was incorporated to systematically evaluate both their individual and collective impacts. The key findings of this study can be summarized as follows:

- The Archie's *m*-exponents in both vertical (m_v) and horizontal (m_h) directions, as well as electrical anisotropy (λ_e), exhibited strong correlations with all the employed particle shape parameters.
- Roundness (RD) demonstrated the strongest statistical significance and predictive power among all parameters, reflecting the ability of RD to capture the electrical tortuosity.
- Simplified regression models using only RD maintained high R^2 values (≥ 0.95), further supporting its dominant influence on electrical properties. Previous experimental results support these findings.

These findings highlight that characterizing particle shape through image-based analysis can improve predictive models for Archie's *m*-exponent, ultimately leading to better interpretation of soil resistivity in geotechnical and environmental applications. To confirm the broader applicability of this approach, validation using additional datasets including field measurements is necessary. In addition, as this study focused exclusively on poorly graded sand, future research should investigate sand with varying amounts of fines and/or well-graded sand. Furthermore, numerical simulations such as the Discrete Element Method (DEM) and coupled Computational Fluid Dynamics–Discrete Element Method (CFD–DEM) could be employed to further investigate and visualize the microstructural interactions between particle shape and electrical conduction behavior under various packing conditions.

CRediT authorship contribution statement

Bosung Choi: Writing – original draft, Investigation, Formal analysis, Data curation. **Jeongwoo Kim:** Methodology, Investigation. **Hyunwook Choo:** Writing – review & editing, Visualization, Investigation, Funding acquisition, Data curation, Conceptualization. **Jongmuk Won:** Visualization, Investigation.

Declaration of competing interest

The authors declare that they have no known competing financial interests or personal relationships that could have appeared to influence the work reported in this paper.

Acknowledgement

This work was supported by the National Research Foundation of Korea (NRF) grant funded by the Korean government (MSIT). RS-2023-00221719

Supplementary materials

Supplementary material associated with this article can be found, in the online version, at doi:10.1016/j.rineng.2025.105794.

Data availability

Data will be made available on request.

References

[1] A. Abd Malik, A. Madun, M.A. Talib, N. Wahab, M.M Dan, Interpretation of soil grain size effect on electrical resistivity method, Phys. Chem. Earth Parts A/B/C. 129 (2023) 103324.
[2] D. Chandrasasi, S.S. Sachro, S. Suharyanto, T.T. Putranto, Employing the vertical electrical soundings (VES) and lithological data for defining the hydrostratigraphic unit in the mud Lapindo disaster area, Results Eng. (2025) 26.
[3] V.A. Franco-Luján, M.A. Maldonado-García, V.G. Jiménez-Quero, P. Montes-García, Hr Reliability of Electrical Resistivity On the Long-Term Monitoring of Concrete, Results Eng, 2023, p. 18.
[4] M.F. Hasan, H. Abuel-Naga, E.-C. Leong, A modified series-parallel electrical resistivity model of saturated sand/clay mixture, Eng. Geol. 290 (2021) 106193.
[5] H. Lee, J.W. Lee, T.M. Oh, Permeability evaluation for artificial single rock fracture according to geometric aperture variation using electrical resistivity, J. Rock Mech. Geotech. Eng. 13 (4) (2021) 787–797.
[6] J.K. Mitchell, K. Soga, Fundamentals of Soil Behavior, John Wiley & Sons, 2005.
[7] A. Samouelian, I. Cousin, A. Tabbagh, A. Bruand, G. Richard, Electrical resistivity survey in soil science: a review, Soil. Tillage Res. 83 (2) (2005) 173–193.
[8] K. Sangprasat, A. Puttiwongrak, S. Inazumi, Comprehensive analysis of correlations between soil electrical resistivity and index geotechnical properties, Results. Eng. (2024) 23.
[9] G.E. Archie, The electrical resistivity log as an aid in determining some reservoir characteristics, Trans. Am. Inst. Min. Metall. Eng. 146 (1942) 54–61.
[10] J.C. Cai, W. Wei, X.Y. Hu, D.A. Wood, Electrical conductivity models in saturated porous media: a review, Earth-Sci. Rev. 171 (2017) 419–433.
[11] H. Choo, S.E. Burns, Review of Archie's equation through theoretical derivation and experimental study on uncoated and hematite coated soils, J. Appl. Geophy. 105 (2014) 225–234.
[12] H. Choo, J. Park, T.T. Do, C. Lee, Estimating the electrical conductivity of clayey soils with varying mineralogy using the index properties of soils, Appl. Clay. Sci. (2022) 217.
[13] P.W.J. Glover, M.J. Hole, J. Pous, A modified Archie's law for two conducting phases, Earth Planet. Sci. Lett. 180 (3–4) (2000) 369–383.
[14] H.S. Salem, Determination of porosity, formation resistivity factor, Archie cementation factor, and pore geometry factor for a glacial aquifer, Energy Sourc. 23 (6) (2001) 589–596.
[15] H.S. Salem, G.V. Chilingarian, The cementation factor of Archie's equation for shaly sandstone reservoirs, J. Pet. Sci. Eng. 23 (2) (1999) 83–93.
[16] J. Won, J.U. Kim, H. Choo, Estimation of the swelling strain and swelling pressure of compacted bentonite using electrical conductivity, Appl. Clay. Sci. (2023) 242.
[17] H. Ko, H. Choo, K. Ji, Effect of temperature on electrical conductivity of soils–Role of surface conduction, Eng. Geol. (2023) 107147.
[18] Y. Chu, S. Liu, B. Bate, L. Xu, Evaluation on expansive performance of the expansive soil using electrical responses, J. Appl. Geophy. 148 (2018) 265–271.
[19] J. Gong, X.W. Pang, Y. Tang, M. Liu, J. Jiang, X.D. Ou, Effects of particle shape, physical properties and particle size distribution on the small-strain stiffness of granular materials: a DEM study, Comput. Geotech. (2024) 165.
[20] C. Guan, C. Zhang, Congying LI, Influence of real particle morphology on single particle crushing behavior of rockfill based on FDEM, J. Rock Mech. Geotech. Eng (2024).
[21] M.H. Hatefi, M. Arabani, M. Payan, P.Z. Ranjbar, S. Keawsawasvong, P. Jamsawang, The role of particle shape in the mechanical behavior of granular soils: a state-of-the-art review, Results Eng. (2024) 24.
[22] G.Y. Hu, B. Zhou, Z.H. Shen, H.B. Wang, W.B. Zheng, A Resolved CFD-DEM Investigation On Granular Sand Sedimentation Considering Realistic Particle Shapes, Geotechnique, 2024.
[23] C. Lee, H.S. Suh, B. Yoon, T.S. Yun, Particle shape effect on thermal conductivity and shear wave velocity in sands, Acta Geotech. 12 (3) (2017) 615–625.
[24] J.C. Santamarina, K.A. Klein, M.A. Fam, Soils and waves: particulate Materials behavior, Characterization and Process Monitoring, J. Wiley & Sons, Chichester, England, 2001.

[25] G.C. Cho, J. Dodds, J.C. Santamarina, Particle shape effects on packing density, stiffness, and strength: natural and crushed sands, J. Geotech. Geoenvironment. Eng. 132 (5) (2006) 591–602.
[26] H. Shin, J.C. Santamarina, Role of particle angularity on the mechanical behavior of granular mixtures, J. Geotech. Geoenvironment. Eng. 139 (2) (2013) 353–355.
[27] J. Yang, X.D. Luo, Exploring the relationship between critical state and particle shape for granular materials, J. Mech. Phys. Solids. 84 (2015) 196–213.
[28] W.D Carrier, Goodbye, Hazen; hello, Kozeny-Carman, J. Geotech. Geoenvironment. Eng. 129 (11) (2003) 1054–1056.
[29] S.J. Rodrigues, N. Vorhauer-Huget, T. Richter, E. Tsotsas, Influence of particle shape on tortuosity of non-spherical particle packed beds, Processes 11 (1) (2022) 3.
[30] J. Won, J. Park, H. Choo, S. Burns, Estimation of saturated hydraulic conductivity of coarse-grained soils using particle shape and electrical resistivity, J. Appl. Geophy. 167 (2019) 19–25.
[31] P.D. Jackson, D. Taylorsmith, P.N. Stanford, Resistivity-porosity-particle shape relationships for marine sands, Geophysics 43 (6) (1978) 1250–1268.
[32] P.N. Sen, Grain shape effects on dielectric and electrical-properties of rocks, Geophysics 49 (5) (1984) 586–587.
[33] M.R.J. Wyllie, A.R. Gregory, Formation factors of unconsolidated porous Media - influence of particle shape and effect of cementation, Trans. Am. Inst. Min. Metall. Eng. 198 (1953) 103–110.
[34] S.J. Blott, K. Pye, Particle shape: a review and new methods of characterization and classification, Sedimentology 55 (1) (2008) 31–63.
[35] J. Zheng, R.D. Hryciw, Traditional soil particle sphericity, roundness and surface roughness by computational geometry, Géotechnique 65 (6) (2015) 494–506.
[36] F. Altuhafi, C. O'Sullivan, I. Cavarretta, Analysis of an image-based method to quantify the size and shape of sand particles, J. Geotech. Geoenvironment. Eng. 139 (8) (2013) 1290–1307.
[37] Y. Yang, Z. Wei, A. Fourie, Y. Chen, B. Zheng, W. Wang, S. Zhuang, Particle shape analysis of tailings using digital image processing, Environ. Sci. Pollut. Res. 26 (2019) 26397–26403.
[38] O.M.Y. Koo, P.W.S. Heng, The influence of microcrystalline cellulose grade on shape and shape distributions of pellets produced by extrusion-spheronization, Chem. Pharm. Bull. 49 (11) (2001) 1383–1387.
[39] C. Mora, A. Kwan, Sphericity, shape factor, and convexity measurement of coarse aggregate for concrete using digital image processing, Cem. Concr. Res. 30 (3) (2000) 351–358.
[40] H.S. Suh, K.Y. Kim, J. Lee, T.S. Yun, Quantification of bulk form and angularity of particle with correlation of shear strength and packing density in sands, Eng. Geol. 220 (2017) 256–265.
[41] H. Wadell, Volume, shape, and roundness of rock particles, J. Geol. 40 (5) (1932) 443–451.
[42] H. Choo, J. Song, W. Lee, C. Lee, Impact of pore water conductivity and porosity on the electrical conductivity of kaolinite, Acta Geotech. 11 (6) (2016) 1419–1429.
[43] J.H. Kim, H.K. Yoon, S.H. Cho, Y.S. Kim, J.S. Lee, Four electrode resistivity probe for porosity evaluation, Geotech. Test. J. 34 (6) (2011) 668–675.
[44] K.A. Klein, J.C. Santamarina, Electrical conductivity in soils: underlying phenomena, J. Eng. Eng. Geophys. 8 (4) (2003) 263–273.
[45] B.S. Nabawy, H.M. Khalil, M.S. Fathy, F. Ali, Impacts of microfacies type on reservoir quality and pore fabric anisotropy of the Nubia sandstone in the central Eastern Desert, Egypt, Geol. J. 55 (6) (2020) 4507–4524.
[46] D. Tiab, E.C. Donaldson, Petrophysics: theory and Practice of Measuring Reservoir Rock and Fluid Transport Properties, Gulf Professional Publishing, 2004.
[47] Shimobe, S., and Moroto, N. (1995) "A new classification chart for sand liquefaction." *Proc., Proc. 1st Int. Conf. on Earthquake Geotech. Engrg.*, Tokyo, 315–320.
[48] H. Choo, W. Lee, C. Lee, S.E. Burns, Estimating porosity and particle size for hydraulic conductivity of binary mixed soils containing two different-sized silica particles, J. Geotech. Geoenvironment. Eng. 144 (1) (2018).
[49] H. Saomoto, J. Katagiri, Particle shape effects on hydraulic and electric tortuosities: a novel empirical tortuosity model based on van Genuchten-Type function, Transp. Porous Media. 107 (3) (2015) 781–798.
[50] D. Kazidenov, Y. Amanbek, Permeability estimation from pore to Darcy in cemented granular media resolved CFD-DEM model, Results Eng. (2024) 24.
[51] B. Ghanbarian, A.G. Hunt, R.P. Ewing, M. Sahimi, Tortuosity in porous Media: a critical review, Soil. Sci. Soc. Am. J. 77 (5) (2013) 1461–1477.